First Semi-Annual Technical Report

July 1, 1970 - January 1, 1971

NEW METHODS FOR GROWTH AND CHARACTERIZATION OF GaAs AND MIXED III-V SEMICONDUCTOR CRYSTALS
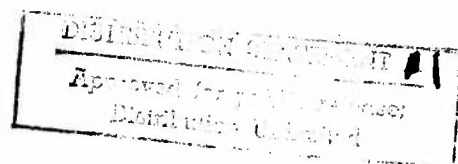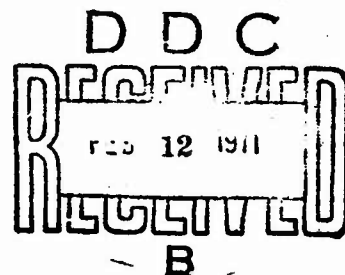
University of Southern California
Los Angeles, California 90007

Submitted to

ADVANCED RESEARCH PROJECTS AGENCY

D D C
RECEIVED
FEB 12 1971
- B -

39

SUMMARY

A new technique for growing bulk gallium arsenide crystals has been invented and is being developed. Potentially this will enable us to routinely produce III-V semiconductor crystals of higher quality than presently available. The evaporation rate of a melt was found to vary with the inverse one-third power of the total pressure, which corresponds to turbulent free convection. A new technique has been developed for drying encapsulating glasses, such as B_2O_3, for use in crystal growth. More rapid drying is obtained than with previous techniques. It has been discovered that surface moisture on vitreous B_2O_3 can easily be removed by merely exposing the material to a vacuum at room temperature.

Improved smoothness of thin films deposited by liquid epitaxial growth was achieved by adding arsenic to the hydrogen atmosphere during growth. $GaAs_{1-x}Sb_x$ and $Ga_{1-x}In_xAs$ alloy films have been grown with x up to 0.13 for In and up to 0.18 for Sb. Vegard's law was found to be valid for $GaAs_{1-x}Sb_x$. Photoluminescence data for these alloys indicated impurity-band transitions. Photoluminescent efficiencies were encouragingly good, i.e., within a factor of 10 of solution-grown GaAs.

An improved polishing technique has been developed using sodium hypochlorite cn a special polishing pad. When used in a special lapping apparatus substrate thicknesses down to 10 micrometers can be obtained. We have developed a technique for producing reliable metal contacts on GaAs. Plating from a molten salt bath is utilized.

An improved method has been developed for interpreting data on photoemission from Schottky barriers. Such results aid in analysis of impurity and interface effects as well as for measuring the barrier height of semiconductors. Theoretical and experimental methods are under development for determining the presence and behavior of deep-lying impurities by use of capacitance-voltage-frequency measurements.

-1-

Gallium arsenide field effect transistors have been produced by our liquid epitaxial growth techniques. Low reverse-biased leakage currents were obtained and found to be associated with a highly-regular substrate-film interface.

The following capital equipment has been purchased under this grant and is now in operation:

Analytical balance

Vacuum pumps (2)

Oven

The vast majority of needed capital equipment has not yet been received.

CONTENTS

I. INTRODUCTION

The purpose of this program is to develop new and improved methods for the growth and characterization of gallium arsenide (GaAs) and mixed III-V semiconductor crystals. The responsible staff are shown in Table I. Related programs at USC are shown in Table II.

Table I
Responsible Staff

Bulk crystal growth - W. Allred

Thin film growth, analyses, and device fabrication - J. Whelan

Schottky barrier and Hall effect characterization - C. Crowell

Dislocation generation and study by X-ray topography and
electrical measurements - R. Wang

Polishing and microwave devices - H. Stover

Table II
Related Programs

Local mode studies of impurities in semiconductors - W. Spitzer

Interaction of electron beams with semiconductors - D. Wittry

Luminescence in semiconductors - M. Gershenzon

Acoustoelectric devices - K. Lakin

Interaction between the staff members in both Table I and Table II is strong and cooperation is outstanding. For convenience in this report we have described separately the progress in each area. Nevertheless it should be emphasized that all are interdependent and have involved cooperative efforts.

II. MATERIALS PREPARATION

A. New Czochralski Technique

A central problem in pulling bulk crystals of gallium arsenide is avoidance of arsenic evaporation from the melt. In the past this has been accomplished by two techniques. In the oldest technique the crucible, crystal, and pull rod were located inside a quartz chamber held at a sufficiently high temperature that condensation of arsenic did not occur on the walls. The pull rod was coupled magnetically to an external drive system which allowed both rotation and vertical motion. Irregular rotation and pulling resulted. To avoid this, the liquid-encapsulated Czochralski technique was developed several years ago. A layer of molten B_2O_3 was placed on the surface of the GaAs melt to prevent evaporation. Crystals were pulled through the B_2O_3. Unfortunately, the B_2O_3 layer blurred the view of the melt-crystal miniscus making control difficult. Molten B_2O_3 also adhered to the crystal and later generated stresses due to differences in thermal expansion.

We have invented and built a Czochralski apparatus[*] which overcomes these difficulties. The new grower, shown schematically in Figure 1, uses a direct drive similar to that used in conventional Ge and Si growers. The smoothness of rotation and pull is limited only by the mechanical system. The pull rod rotates through a B_2O_3 or other liquid seal in a close-fitted tube. The molten glass is necessary to prevent the loss of arsenic from the pulling chamber during growth. It is the use of the push-pull rotating seal (which can operate at $600^{\circ}C$ and above) which allows the magnetic puller to be replaced. Since the B_2O_3 is not in contact with the GaAs, as in liquid encapsulated growth, it is not necessary to start with pre-reacted GaAs. Gallium and arsenic in stoichiometric amounts are simply inserted into the crucible and reacted in situ. The construction of the new system involves only simple glass-

---

[*] Patent to be applied for.

-5-

VACUUM

ROTATING ROD

B_2O_3 SEAL

RESISTANCE HEATER (I)

QUARTZ CHAMBER

RESISTANCE HEATER (II)

GRAPHITE CRUCIBLE

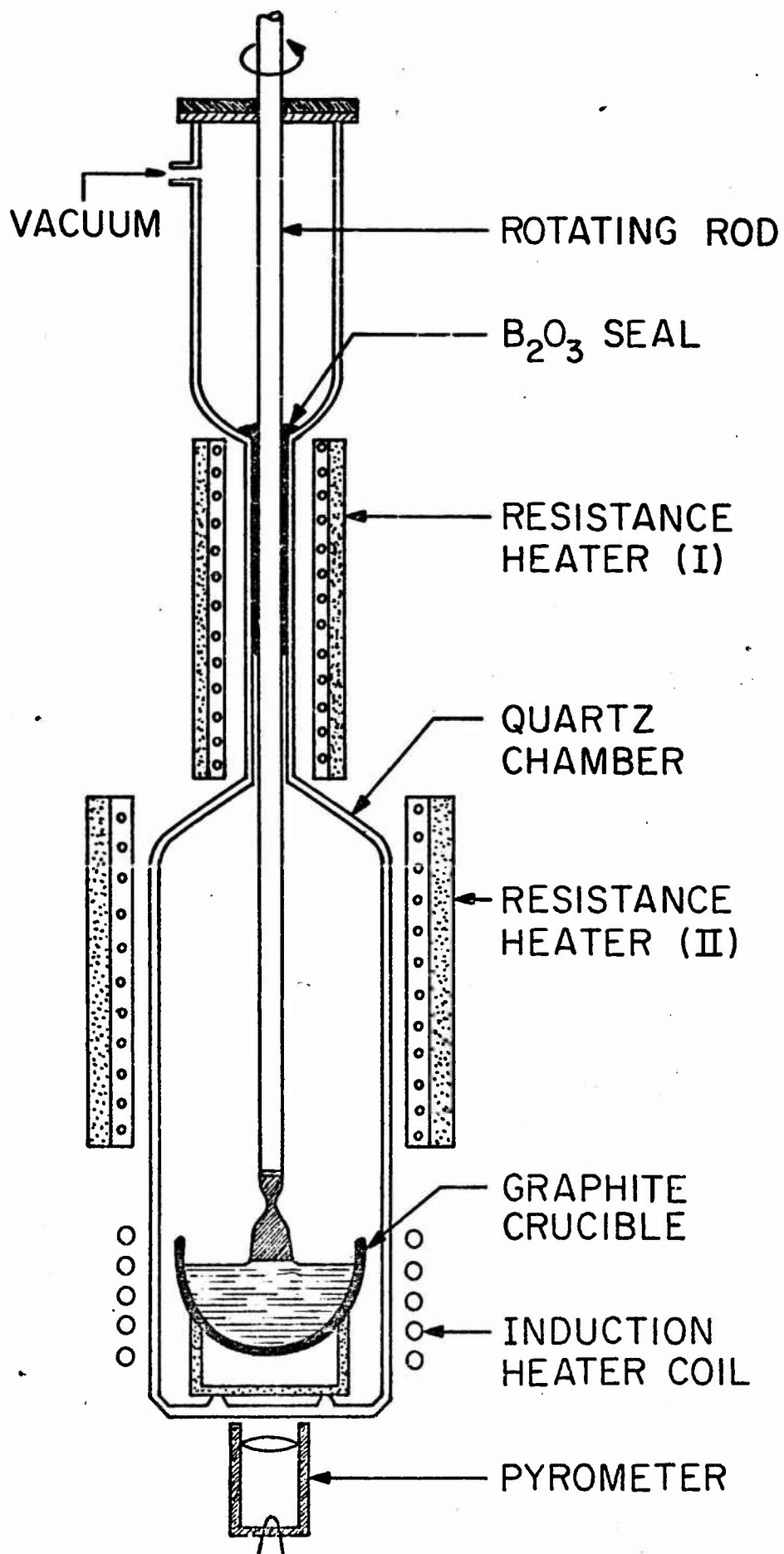INDUCTION HEATER COIL

PYROMETER

Fig. 1   New Czochralski Apparatus

blowing, with no precision quartz or glass-blowing required.

Preliminary tests have proven the validity of the concepts of this
new technique. Several attempts have been made to grow single crystals
of GaAs in the new grower. At the onset of the work a problem of arsenic
leakage through the B_2O_3 seal was encountered. This was caused by
water which was present in the B_2O_3. The water reacted with the
arsenic vapor to form an oxide which dissolved in the B_2O_3 and was
readily transported through the seal to the vacuum chamber above. The
problem was solved by heating the B_2O_3 in a vacuum within the system,
thus preventing pick-up of H_2O during the loading process. The B_2O_3
was further purified by first bleeding dry helium into the pulling chamber
before melting of the B_2O_3 and then passing the helium up through the
molten B_2O_3 at $900^{\circ}C$. This process was very effective in removing
residual water bubbles from the B_2O_3.

Arsenic leakage was also caused by channeling of the B_2O_3. The
channels were formed when the pull rod was pushed down into the pulling
chamber. The B_2O_3 tended to run down only one side of the pull rod,
leaving a void on the other side, permitting loss of arsenic. The
channeling was eliminated by using helium pressure to push the B_2O_3
down around the pull rod in an even manner. Subsequent runs have
resulted in no arsenic loss through the B_2O_3 seal. Several runs have
been made to resolve other problems unrelated to the rotating seal. The
only problem yet to be corrected is that of adequate temperature control.
This problem was caused by a malfunction of the induction heater control
unit. In spite of the poor temperature control two GaAs single crystals
were grown. We have hopes that this new technique will permit routine
growth of GaAs of much higher perfection than presently available.

B. Liquid-Encapsulated Floating-Zone Melting

In all of the Czochralski techniques just described, the melt is
contained in a crucible and so is contaminated somewhat by the crucible

-6-

material. Silicon also appears to be transported from the quartz container. We propose to avoid these difficulties by development of liquid-encapsulated floating-zone melting. The apparatus design is shown in Figure 2. The melt will contact only B_2O_3 or another encapsulant, which will not only prevent evaporation but should also act as a getter for impurities. We therefore expect to be able to produce bulk GaAs of higher purity and higher mobilities than produced previously. An encapsulant with a density near that of molten GaAs would permit zone melting of large ingots.

We have completed the design of this apparatus and have begun construction. In the future, we plan to complete the apparatus and test it first on GaAs with B_2O_3 as an encapsulant. Other encapsulants of higher density will then be sought. Mixed III-V material will eventually be treated.

C. Drying of Encapsulants

As noted above, it is important to remove traces of moisture from the encapsulant to avoid reaction with the semiconductor melt and vapors. Previous techniques for drying B_2O_3 utilized long exposure to high vacuums at elevated temperature. The initial heating produced troublesome frothing. Addition of reactive metals has been employed to hasten drying. We have developed a new drying technique that is rapid and requires no addition of reactive metals.

In this new technique Boric anhydride (B_2O_3) powder is charged into a carbon crucible about 2/3 full, and slowly heated in dry nitrogen gas at one atmosphere. When the frothing begins, at a temperature of 700 to 800°C, the bubbles are broken with a rod. When the formation of bubbles subsides sufficiently, the temperature is again slowly raised up to 1200°C. During this period, bubbling of dry N_2 gas through the B_2O_3 melt is started. Dry gas is not effective below 1000°C because the gas flows through a channel formed in B_2O_3 due to the high viscosity

-7-

VACUUM TUBE

COOLING WATER
JACKET

QUARTZ TUBE

FURNACE (1)

MOLTEN B_2O_3
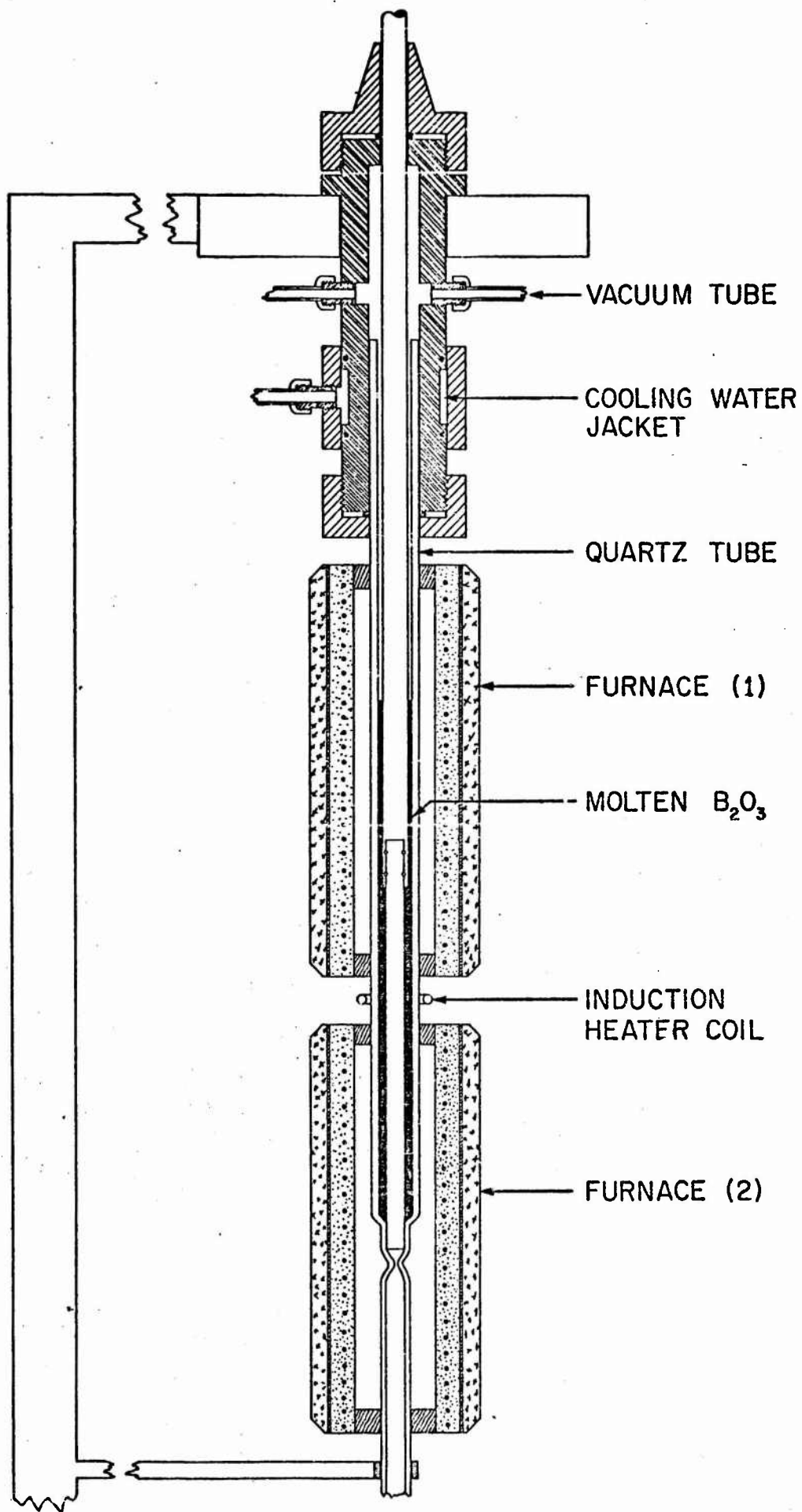
INDUCTION
HEATER COIL

FURNACE (2)

Figure 2. Preliminary Design of Liquid-Encapsulated Floating-Zone Melting Apparatus

of the melt. Around a temperature of $1200^{\circ}C$, good bubbles are formed and agitate the melt very vigorously. The dry gas bubbles not only entrain the gases produced in the melt, but also accelerate the rate of mass transfer by continuous renewal of the interfaces of carbon-B_2O_3, and dry gas-B_2O_3.

Chemical reaction between the carbon of the crucible wall and H_2O in B_2O_3 is expected to take place above $1000^{\circ}C$. For example, Poch [1] dried B_2O_3 in a vacuum by the following consecutive steps.

(i) 12 hours in a platinum crucible (shallow) at $850^{\circ}C$
and 1 atmosphere.

(ii) 5 hours in a platinum crucible at $1300^{\circ}C$ and 1 Torr.

(iii) 6 hours in carbon crucible at $1300^{\circ}C/1$ Torr.

The minimum H_2O content attained by the above method was 10 ppm by weight, which is the lowest value found in the literature.

After completion of drying by our technique the melt is cooled very slowly in order to avoid the formation of suspended gas bubbles in the solid B_2O_3.

We are attempting to develop a technique for determining trace water in fused B_2O_3 by infrared transmission measurements. Sheets of B_2O_3 were slowly pulled from the melt both preceding and following drying. To calibrate the infrared absorption some of the sheets were exposed to moist air. The amount of moisture introduced was determined by weighing the samples. Typical infrared transmission curves are shown in Figure 3. It may be seen that water was responsible for two different bands in B_2O_3, one at $2.84\,\mu$ and one at $3.13\,\mu$. The $3.13\,\mu$ absorption was increased by exposure of samples to moist air while the $2.84\,\mu$ band was not significantly altered. Exposure to a vacuum at room temperature caused the $3.13\,\mu$ transmission to slowly increase until it was the same as before exposure to humid air. The $2.84\,\mu$ band was unaffected by vacuum. Thus it was concluded that bulk moisture was
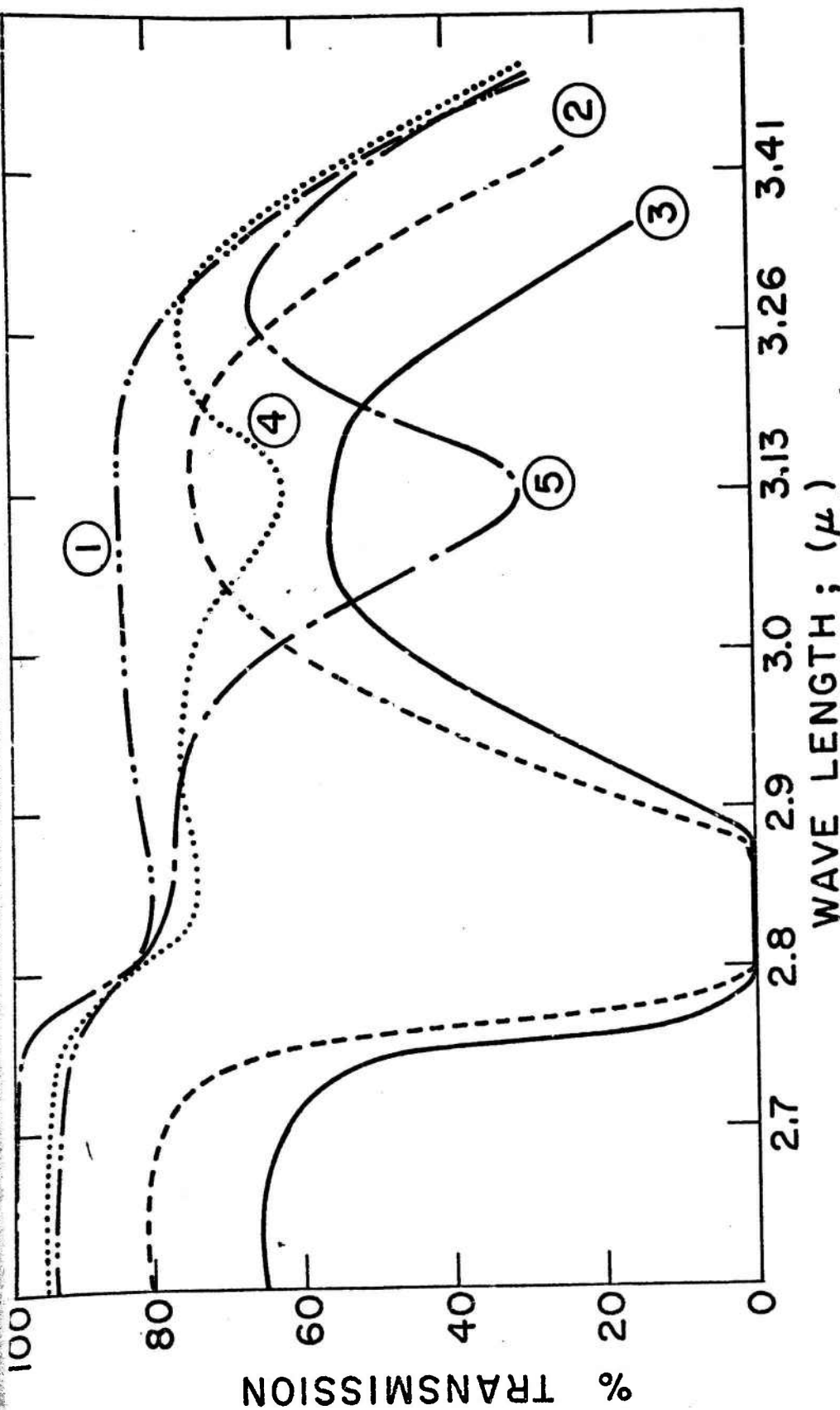
-8-

Figure 3. Infrared Transmission curves for vitreous boron oxide samples

Curve 1: Dried by bubbling dry N_2 at 1200°C for 10 hours.

0.114 mm thick

Curve 2: Heated at 900°C for 1 hour. 0.259 mm thick

Curve 3: Dry N_2 bubbled through for 1 hour at 950°C. 0.528 mm thick

Curve 4: Dried sample with 0.011 wt. % surface moisture.

0.104 mm thick

Curve 5: Dried sample with 0.038 wt. % surface moisture.

responsible for absorption at 2.84μ while surface moisture was responsible for infrared absorption at 3.13μ . We plan to continue our efforts to develop a method for quantitatively analyzing for trace water in fused B_2O_3.
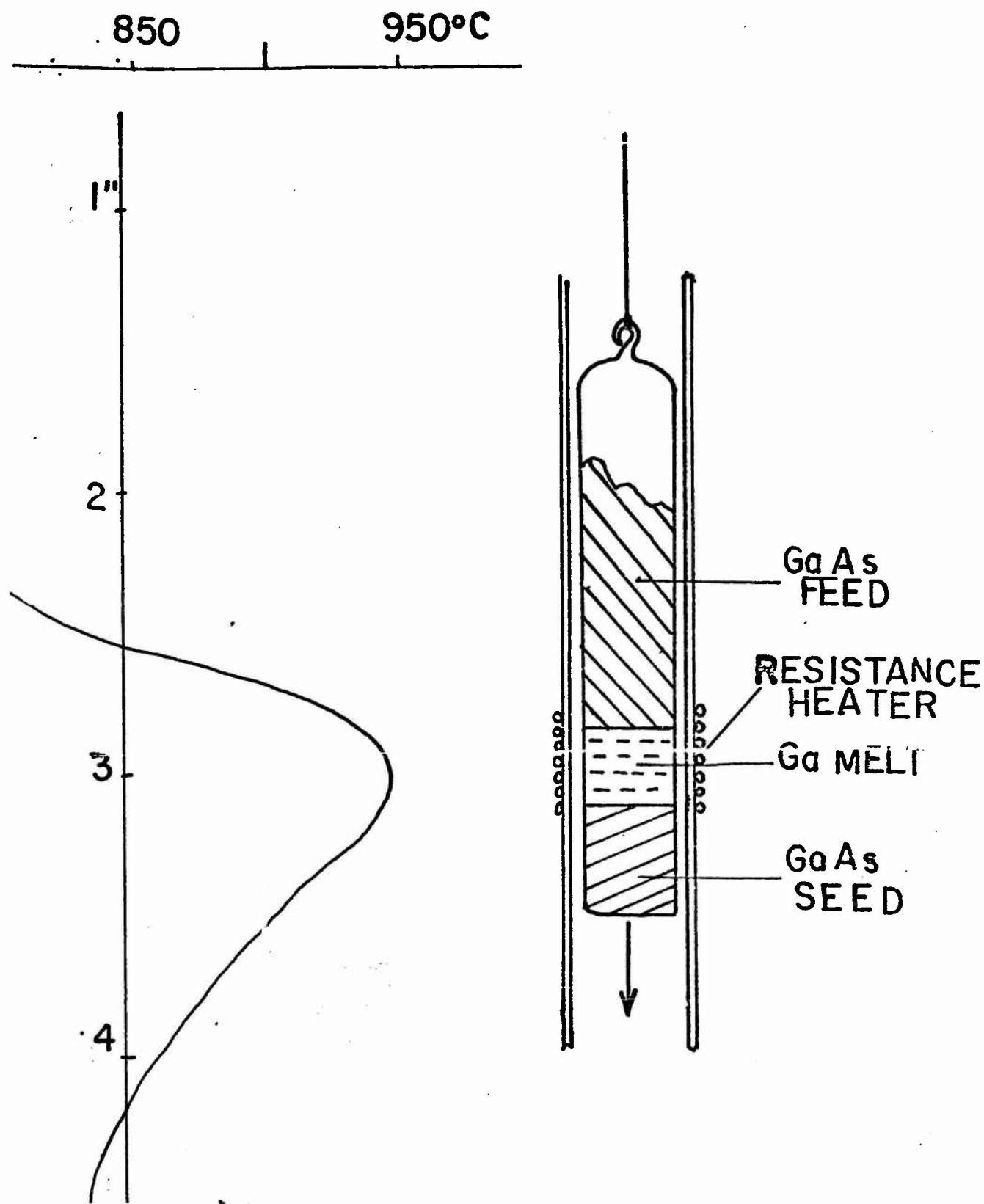
D. Travelling-Heater Method

In the travelling heater method (THM), a solvent zone is slowly moved through solid feed material by movement of a heater, as in Fig. 4. Because of the solvent the temperatures are much lower than when melt growth techniques are utilized. This greatly lessens problems with attack of the container, with vaporization of volatile components, and with thermal strain and resultant defect formation. The zone leveling configuration also makes possible growth of mixed III-V crystals without the composition gradients produced in the normal freezing methods (e.g., Czochralski and Bridgman techniques).

Previous work, primarily at Tyco Laboratories, has demonstrated the feasibility of THM for growth of compounds and mixed crystals. Very little has been published on the phenomena governing THM crystal growth or on the properties of the materials produced thereby. We intend to fill these gaps in crystal growth knowledge, and thereby to enable growth of better crystals. At the present time we feel that we have just about come abreast of the current state of the art on THM growth[2]. Single crystals of GaAs can routinely be produced both with and without seeding, although occasionally polycrystalline ingots are obtained. Figure 5 shows that crystal perfection is improved by THM growth. Our polycrystalline ingots are not homogeneous, as shown by the electron microprobe scans of Figure 6.

E. Liquid Epitaxial Growth

The liquid epitaxial growth technique for producing thin films represents the only crystal growth method that was under investigation

850   950°C

1"

2

3

4

Temperature profile in empty

heating chamber.

GaAs
FEED

RESISTANCE
HEATER

Ga MELT

GaAs
SEED

Figure 4. Travelling Heater Method Apparatus.
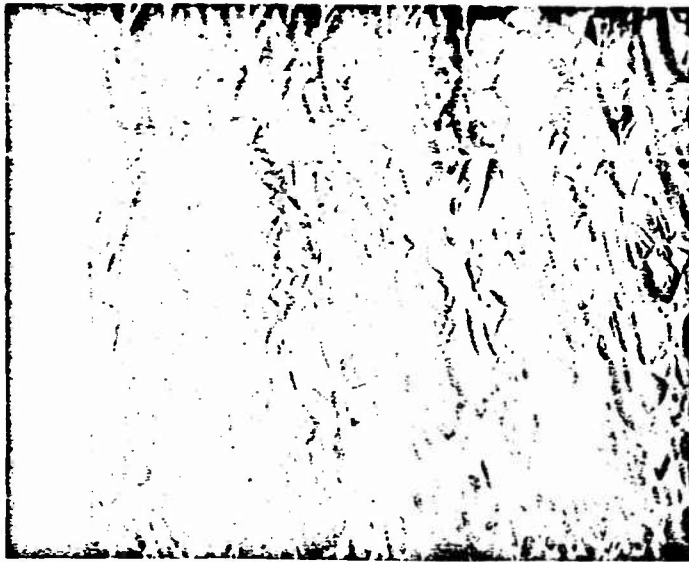
NOT REPRODUCIBLE

A.   Melt grown seed
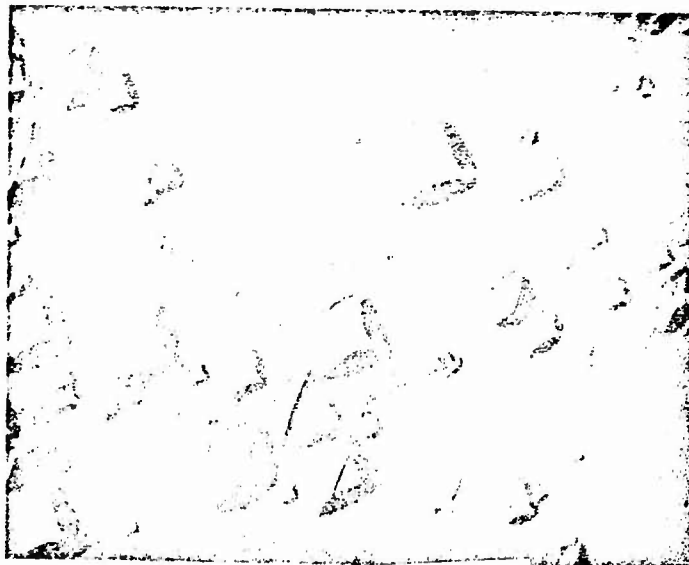
NOT REPRODUCIBLE

B.   THM grown crystal

Figure 5. Ga (111) etch pits

LINEAR SCAN

NOT REPRODUCIBLE

A.   Cathodoluminescence

Te XRAY SPECTRU

BRIGHTNESS

NOT REPRODUCIBLE

B.   Scans of tellurium X-ray spectrum and cathodoluminescence

brightness

Figure 6. Electron microprobe results on THM GaAs

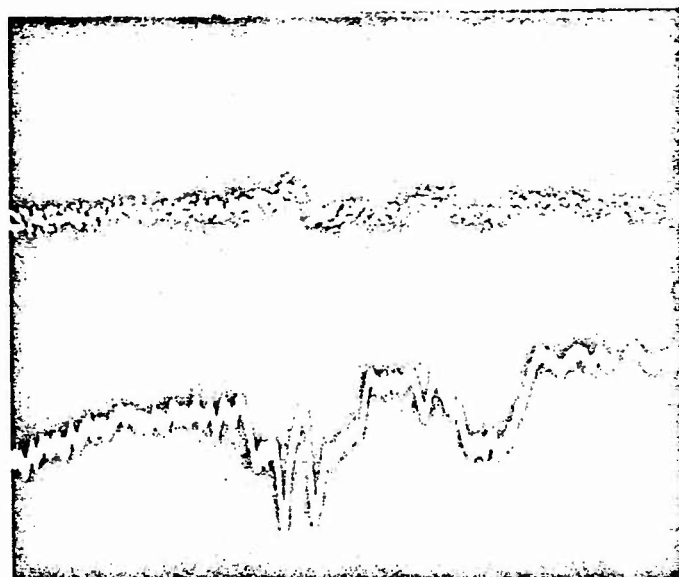at USC before initiation of the present grant. During the report period the surface texture and substrate-interface regularity was significantly improved by the addition of arsenic to the hydrogen atmosphere under which the solution growth occurs. This permitted the growth of smooth films on substrates with the desired orientations, (211) and (311) and moderate dislocation densities, $\sim 5000 \text{ cm}^{-2}$. Comparable results were previously obtainable only with substrates with dislocation densities $\simeq 100 \text{ cm}^{-2}$. (Smoothness is one factor which will ultimately limit the types of devices that can be fabricated from GaAs.)

Variables affecting the characteristics of thin alloy films on GaAs substrates were elucidated. These included the determination of the Ga-In-As liquidus-solidus curve at 860°C, evaluation of film quality as a function of the substrate orientation and a comparison in the nucleation characteristics of the two alloy systems. GaAs substrates with (111) orientations were superior to all other orientations tried, (100), (110), (211) and (311). The density of nucleation ceters was markedly greater for the $GaAs_{1-x}Sb_x$ alloys than for the $Ga_{1-x}In_xAs$ ones. For this reason the $GaAs_{1-x}Sb_x$ alloys are more likely to be useful when films $\sim 1\mu m$ thick are required with energy gaps more than 0.04 eV less than GaAs.

The dependence of lattice constant on composition of $GaAs_{1-x}Sb_x$ alloys has been measured. A linear variation with x was found, corresponding to Vegard's Law. Previous data had indicated a strong deviation from a linear variation. The new results are attributed to the improved homogeneity of our solution-grown alloy films.

One remaining difficulty is the reduction of oxides on the substrate surface prior to growth. An apparatus has been designed for doing this by using a biased zirconia tube as a crucible-oxygen pump. Reduction of oxygen levels in the growth system would permit growth at lower temperatures. This in turn would reduce the contamination problem and simplify thickness control.

F. Related Crystal Growth Programs

In III-V semiconductor crystal growth from the melt, vaporization of one component is usually a troublesome problem. One means of reducing the evaporation rate is to increase the total gas pressure over the melt. In order to test the effectiveness of this method, a study of the evaporation of NaCl melts as a function of pressure was undertaken in cooperation with researchers at Sandia Laboratories in Albuquerque, New Mexico[3]. The theoretical portion of the work was executed at USC.

The evaporation rate of molten NaCl was measured at pressures between 0.74 and 212 psia. In induction-heated crucibles the rate was a linear function of $(1/P)^{1/3}$, with different slopes at high and low pressures. The $(1/P)^{1/3}$ dependence was shown to be expected for turbulent free-convective mass transport. Under some conditions the evaporation rate decreased with decreasing pressures. This observation was attributed to condensation of NaCl in the gas with NaCl particles being carried back into the melt by a reflux process. The large difference in evaporation rates between Ar, He, and CO_2 was attributed not only to differences in thermal conductivity but also to infrared absorption by the CO_2.

Twins are a frequent defect in semiconductor crystals, but nonetheless are of uncertain and mysterious origin. In order to improve our understanding of twin formation, twinning of KBr during solution growth was studied[4]. Large numbers of [211] penetration twins were formed when KBr reagent from one supplier was crystallized from water by evaporation. Most of these were butterfly twins while a few were interpenetrating cubes. Some lots of reagent from another supplier also produced twins while other lots did not. The nontwinning KBr was of an overall higher purity than that which produced twins. Twin formation appeared to be stimulated by Na^+, Cl^-, and Thiazine Red R. Trace amounts of $PbCl_2$ prevented twinning. The maximum yield of twins was obtained at intermediate growth rates. The interface surface was not a

-11-

twin plane but varied widely in orientation. A model showed that the twin intersection forms a step much like that of a screw dislocation at the tip of the butterflies. Experimentally it was found that growth layers originated from this tip and later coalesced to form large waves which trapped tubular inclusions.

G. Lapping and Polishing

Mere growth of bulk crystals is not sufficient either for characterization or for device fabrication. Properly oriented slices with parallel damage-free surfaces are usually required. We have developed improvements over previous techniques for lapping and polishing GaAs slices. A brief discussion follows, with details available upon request.

Abrasive polishing inevitably results in a crystallographically damaged surfaces, although the surface may appear optically perfect. Purely chemical polishes remove damage but generally result in rounded and/or rippled surfaces which are unsatisfactory for many applications. The best method is combined chemical-mechanical polishing. In this technique wafers are rubbed against a soft cloth, paper, or synthetic such as corfam saturated with a very slow chemical etchant. Removal rates typically range from 0.1 to 1 mil/hour. The resulting flat surface can be damage and strain-free.

Three chemical-mechanical polishing systems have been tested and improved at USC. The Syton® system utilizes a colloidal suspension of ~ 25 mμ SiO_2 particles in a pH9.5 aqueous solution[5]. The surface finish produced thereby on GaAs wafers was inferior to the two other methods tested. In addition, the polishing time was longer and more abrasive pre-polishing steps were required.

The use of a solution of 0.05% bromine in methanol for chemical-

---

® Registered trademark of Monsanto Chemical Co.

-12-

mechanical polishing was first described by Sullivan and Kolf[6]. This solution emits noxious and corrosive fumes. Thus a special vented polishing apparatus was constructed of plastic. After a preliminary abrasive polish, a mirror-like surface was obtained in 1 1/2 to 2 hours. It was found unnecessary to place a light source behind the polishing wheel as recommended in Ref. 6. In addition, the polishing wheel was horizontal, rather than inclined as in Ref. 6.

One group at USC favors the bromine-methanol polish while others prefer our recent modification of the sodium hypochlorite (NaOCl) method of Reisman and Rohr[7]. A freshly prepared solution of 15 parts H_2O to 1 part 5% NaOCl was fed at the rate of 300 cc/hour to a Buehler polishing machine. The 8 inch O. D. wheel was covered with a Geoscience Polytex Pix polishing pad. (The polishing cloth used in Ref. 7 was rapidly attacked by the solution.) Dispensing the solutions in bursts, as in Ref. 7, was not found to be necessary. It was necessary to shut off the NaOCl solution flow and flush with water for a few minutes prior to removing the wafers in order to prevent formation of a surface haze.

Very thin wafers for microwave device substrates are desireable both because this reduces the parasitic electrical series resistance and because the removal of heat is enhanced. We can now routinely prepare substrates of thicknesses down to 10μ by use of the NaOCl chemical-mechanical process in combination with a special lapping machine which holds the wafers precisely parallel to the wheel.

III. CHARACTERIZATION

A. Dislocation Studies

Dislocations are introduced during crystal growth and are known to influence the semiconducting properties of the crystal. Unfortunately, a great deal is unknown both about dislocation generation during growth and about their electrical effects. We have undertaken to fill these gaps in our knowledge.

In order to obtain plastic deformation on the $\{111\} < 110 >$ slip system, Czochralski grown GaAs crystals were shaped into thin wafers whose $< 110 >$ slip direction was inclined at 45° to the crystal surface. A 4-point bending jig was designed in order to introduce a uniform distribution of dislocations between the inner knife edges. Good bent crystals were obtained at $700^{\circ}C$ under argon.

The dislocations on the Ga $[111]$ face were revealed by Schell's etchant (mixture of HNO_3 and H_2O). The dislocations on the As $[111]$ face could only be seen when some active agents were added. We found that addition of $1\% AgNO_3$ caused dislocation pits to develop on both Ga- and As faces. X-ray topographic equipment has been ordered and is expected momentarily. This will enable us to confirm the types of dislocations and to see the dislocation networks.

B. Hall Effect Apparatus

A flexible Hall effect system has been designed to provide improved diagnostic measurements. The system will use a variable temperature top loading dewar system for the temperature range $4^{\circ}K$ to $300^{\circ}K$ and will feature a high sensitivity, high impedance ($\approx 10^{12} \Omega$) differential amplifier with capacitive degeneration in the input circuitry. The components for this system and the dewar have be n received. Completion of the construction of the system is anticipated during the next six months.

-14-

C. Tunnel and Thermal Effects in Photoemission from Schottky Barriers

Photoexcitation of carriers from a metal into a Schottky barrier depletion region has been recognized as providing the most direct and unequivocal measure of the barrier height. As such, it affords a prime diagnostic tool for analysis of impurity and interface effects in experimental semiconductor materials. Because of this we have been investigating two sources of error in interpreting these measurements[8]. In principle, such data should be analyzed by use of a Fowler plot[9]. It has been more customary, however, to choose an easier approximate curve fitting technique. A plot of $R^{\frac{1}{2}}$ (photoresponse per absorbed photon)$^{\frac{1}{2}}$ versus photon energy, becomes nearly linear when $h\nu - \varphi_B \gg kT$ (cf., Fig. 7). The intercept of the asymptotic curve occurs when $h\nu = \varphi_B$ within the framework of the Fowler model. In Fig. 8 we show a simple universal curve which can be used to correct the approximate curve fitting procedure. This procedure in effect allows for photoexcitation of electrons in the Fermi tail of the electron distribution in the metal and eliminates the cut and try associated with the Fowler curve fitting procedure.

The above approach is also a useful way to express the corrections associated with photon assisted tunneling through or over a Schottky barrier. We have evaluated these corrections by appropriately weighting the photoexcited electron distribution with transmission coefficients obtained by a computer analysis using techniques similar to those of Crowell and Sze[10]. The model used for the transmission coefficient incorporates image force effects. Thomas-Fermi field penetration into the metal, effective mass differences in the metal and semiconductor conservation of transverse crystal momentum and effects of total band bending in the semiconductor. Results for selected doping and band bending for metal n-type GaAs systems are shown in Fig. 9. Due to the small effective mass of electrons in GaAs these corrections become appreciable for doping $\approx 10^{18} cm^{-3}$. These data provide the corrections to the image
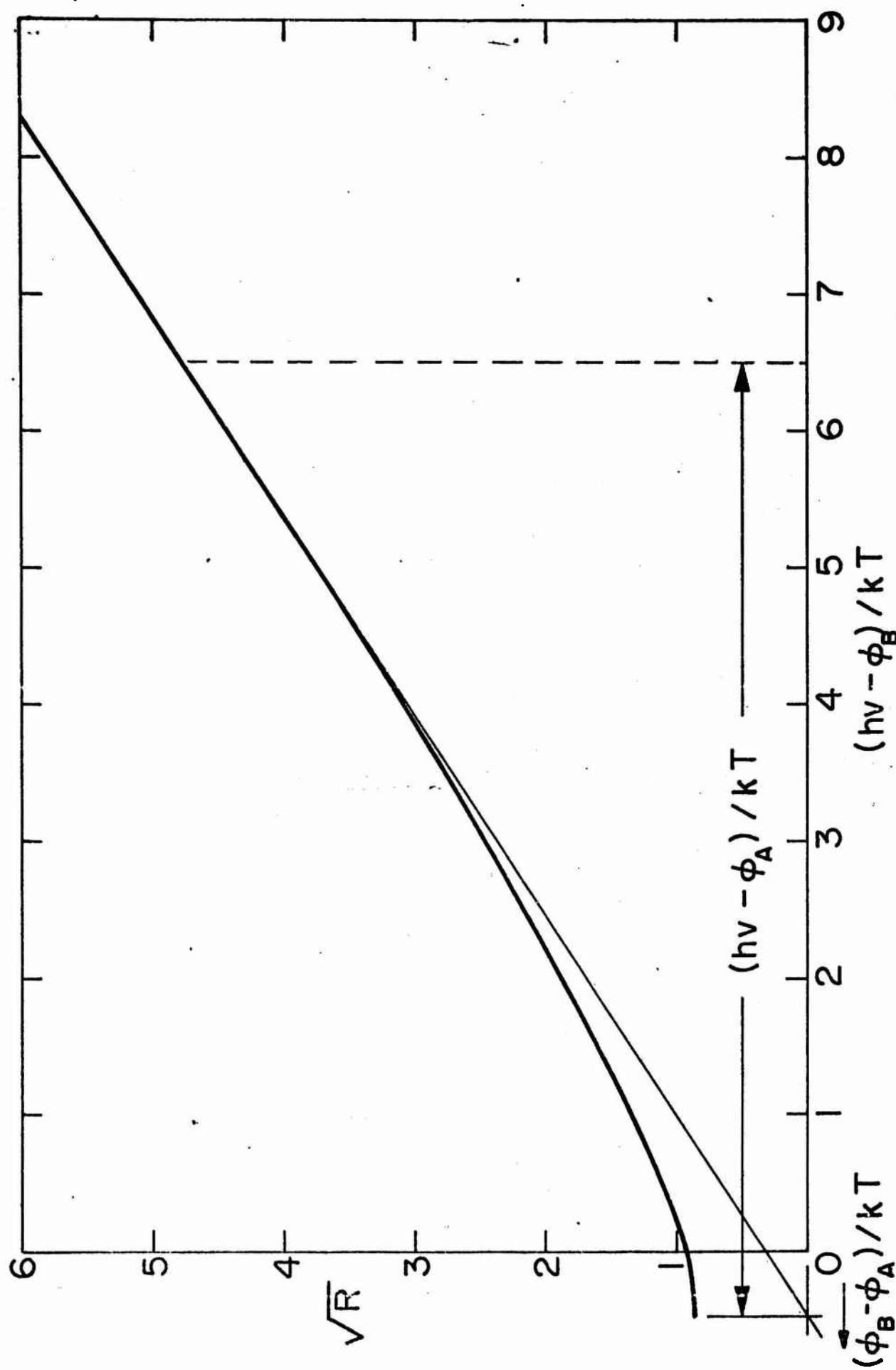
Figure 7. (Photoresponse per absorbed photon)$^{\frac{1}{2}}$ versus (photon energy-barrier height) in units of kT according to the Fowler[9] theory and construction fo find the apparent barrier height at given photon energy.
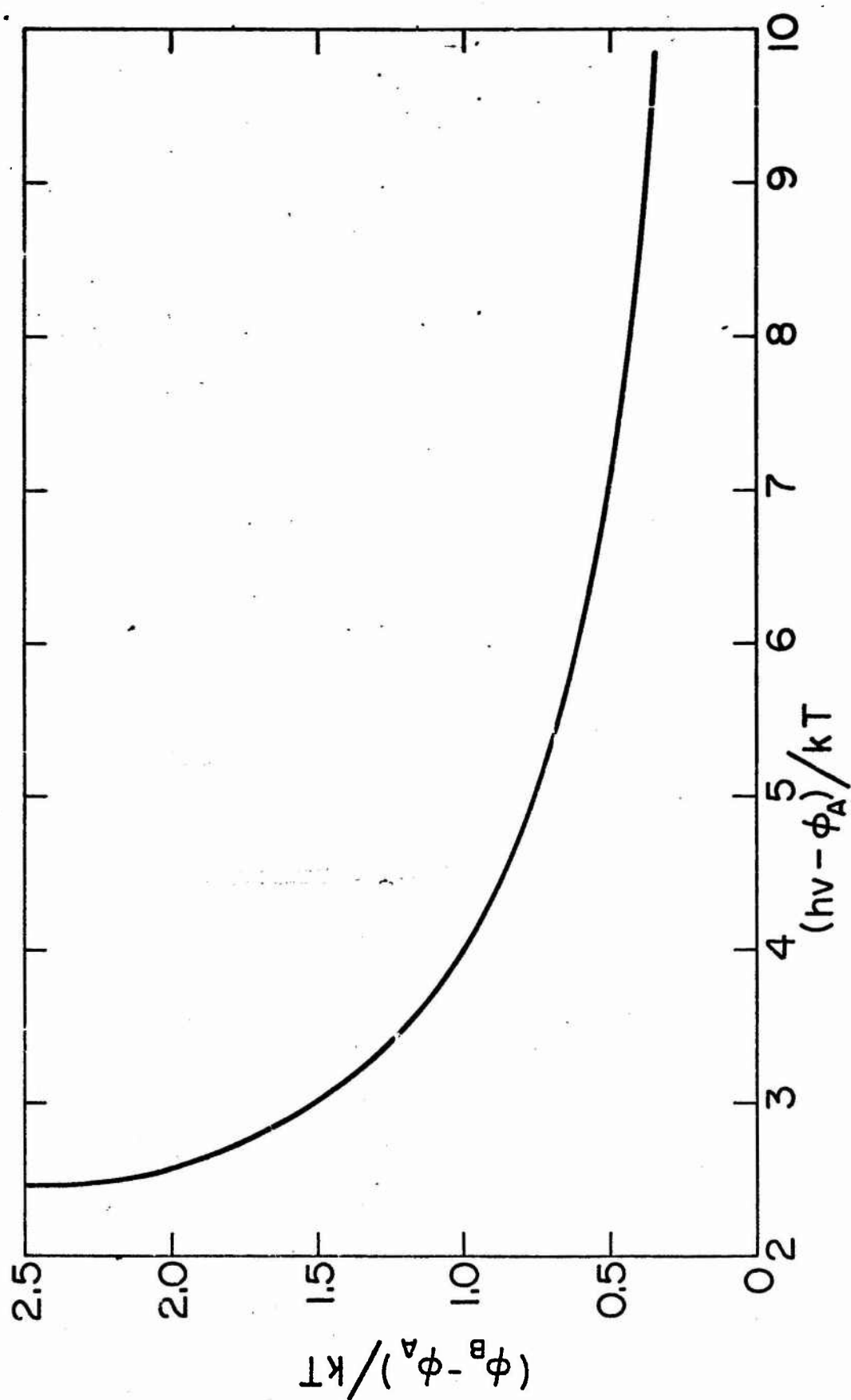
Figure 8. Relationship between apparent and true barrier height versus $(h\nu - q\varphi_A)$ all in units of kT.
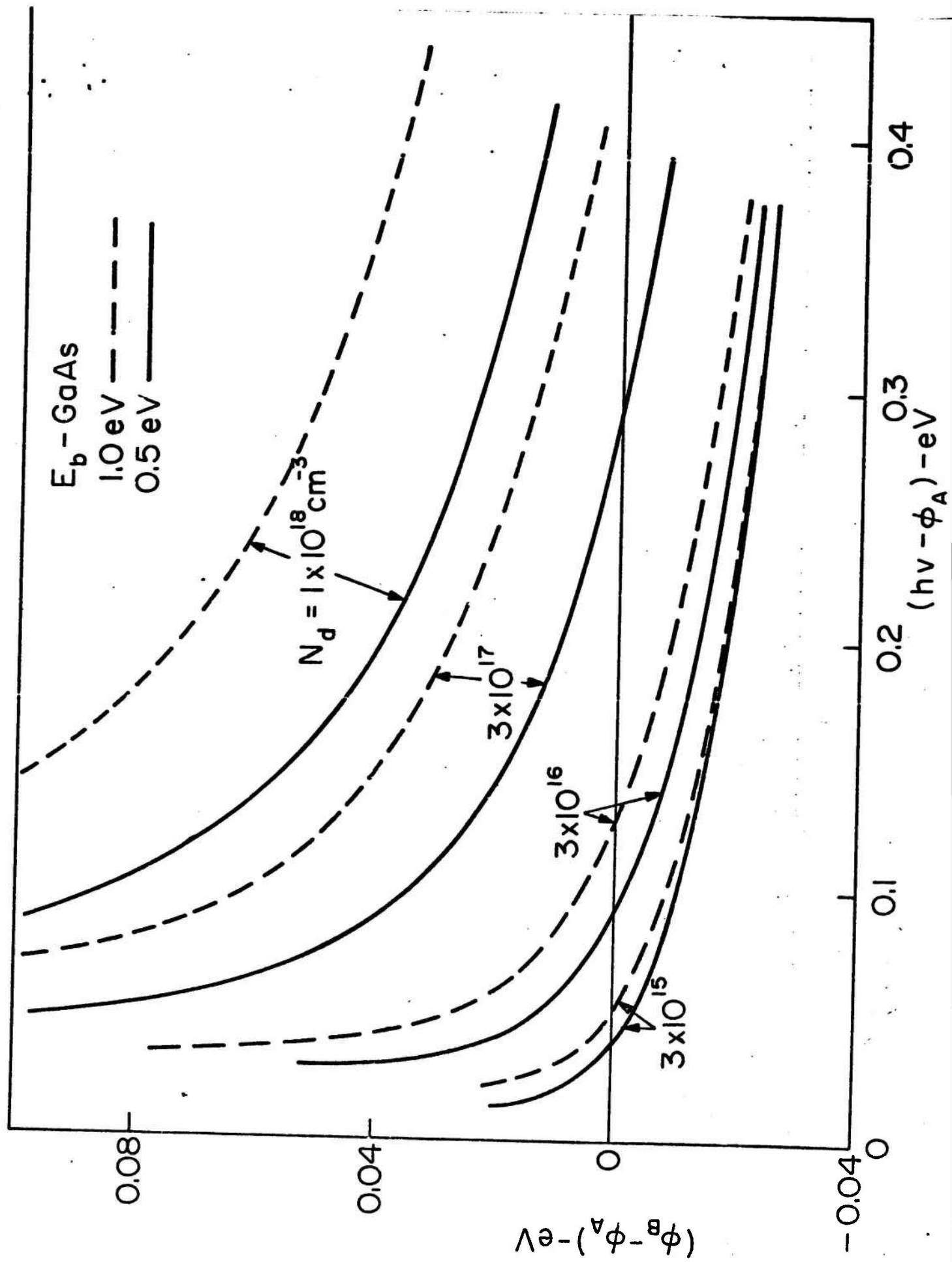
Figure 9. Correction to apparent barrier height due to tunneling for a free
electron metal - n-type GaAs system.

force lowered barriers. The corresponding results for Si show smaller contributions due to tunneling but an appreciable effect due to conservation of transverse momentum which makes the "exact" results come closer to W.K.B. calculations. This work will shortly be submitted for publication.

D. Capacitance Effects of Deep Level Impurities in Schottky Barriers

Deep-level impurities in semiconductors have many undesirable effects and are most frequently found in new semiconducting materials and in lightly doped materials. The nature of their intrinsic behavior has not in general been well defined, especially in the area of capcitance effects. We seek to clarify this problem so that the interference of deep level impurities on capacitance impurity profiles can be more clearly diagnosed and the energy levels and capture cross sections of the deep levels themselves can be determined comparatively in Schottky barrier systems. We plan to use guidelines established by a program of investigation on Si Schottky barriers (funded by the Army Research Office, Durham) in investigations of III-V semiconductors. The following theoretical results were obtained using Joint Services Electronics Program and ARPA support during the initial stages[11].

A typical Schottky barrier energy band diagram is shown in Fig. 10 where one deep donor and one shallow donor level are present. The deep level is ionized mainly when above the bulk Fermi line. The charge density increment for an incremental change in surface potential is also shown. At zero frequency, the center of charge (or effective capcitance spacing) is shown schematically by x_{dc}. At a frequency ω, however, the dotted portion of this distribution does not respond and the effective capacitance spacing becomes x_ω. At high enough frequencies that the deep level cannot respond the spacing becomes $x_{\omega h}$ which is determined by the free electron density in the conduction band. If we assume the validity of Schokley-Read recombination statistics,
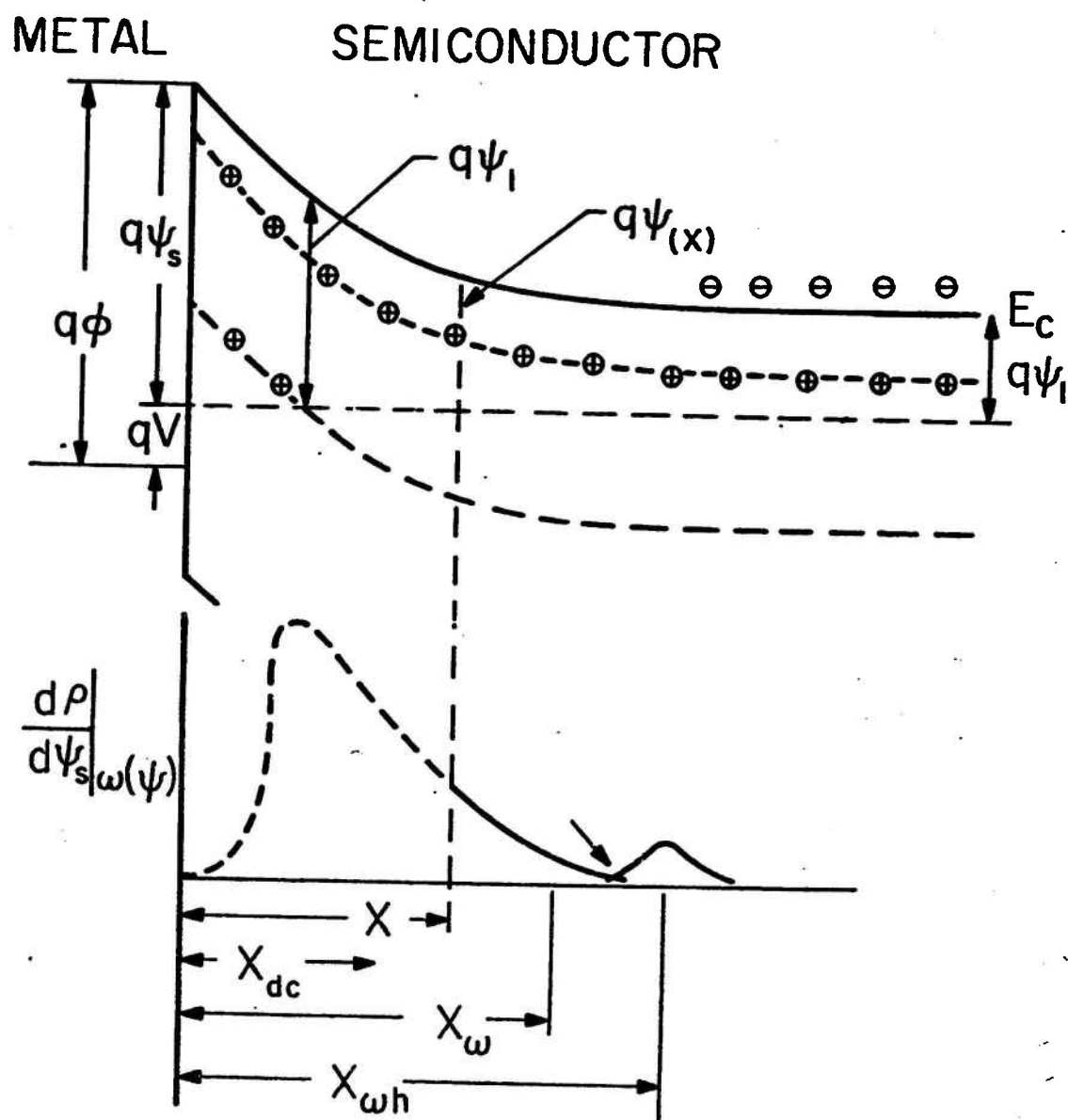
-16-

Figure 10. Electron energy band diagram for Schottky barrier with deep and shallow level impurities plus schematic illustration of geometrical distribution of charge increments for d-c voltage increments (solid plus dashed line) and a voltage increment at frequency $\omega(\psi)$.

$$\omega = \omega(\psi) = \sigma v(n(\psi) + n_1(\psi_i))$$

where σ is the capture cross section for electrons, v the electron thermal velocity and $n(\psi)$ the electron density where the electron potential energy is $q\psi$ relative to the bulk fermi energy ($\omega_1 \equiv \sigma v n_1(\psi_i)$). If we assume that at $\omega(\psi)$ only charges beyond x respond, then the frequency dependence of the capcitance $C(\omega, \psi_s)$ can be expressed in terms of the low frequency (d.c.) variable as follows:

$$\frac{1}{c(\omega, \psi_s)} - \frac{1}{c(0, \psi_s)} = \int_{\omega_s}^{\omega} \frac{1}{c(0, \psi)} \frac{d \ln \rho}{d\psi} \frac{d\psi}{d\omega} d\omega$$

Figure 11 shows the theoretical results in a form which applies for any bias such that $\psi_s >> \psi_i$. The parameter $C_D \left(\equiv \left[\frac{\epsilon q^2(N_D d + N_s)}{kT} \right]^{\frac{1}{2}} \right)$ can be obtained from the slope of $1/C^2$ versus V and the other three parameters which define the system are degree of freeze-out of the deep level $(q(\psi_i - \psi_f)/kT)$, ratio of deep to shallow impurity concentrations, N_s/N_{d_d} for donors or $((N_s/N_{a_d}) - 1)$ for acceptors, and ω_1 the lowest frequency at which all deep level impurities respond. The dotted line shows an asymptotic result due to Schibli and Milnes[12] which is in error by a factor of 4 in elastance difference or a factor of 16 in capture cross section. The effects of freeze-out and ratio of shallow to deep impurity concentrations are far from orthogonal. Accordingly to arsist in diagnosis, the frequency at which 90% of the transition has occurred, ω_9, has been chosen as additional parameter. Figure 12 shows the relationships between $C_D/C(0, \psi_s) - C_D/C(0, \psi_s)$ and ω_9/ω_1 as a function of N_s/N_D. Note that for a given elastance difference the frequency range defines a unique value of N_s/N_D and degree of freeze-out as long as N_s/N_D is not in the region of unity.

The above results show for the first time a method of deducing capture cross section, impurity energy level and ratio of shallow to deep
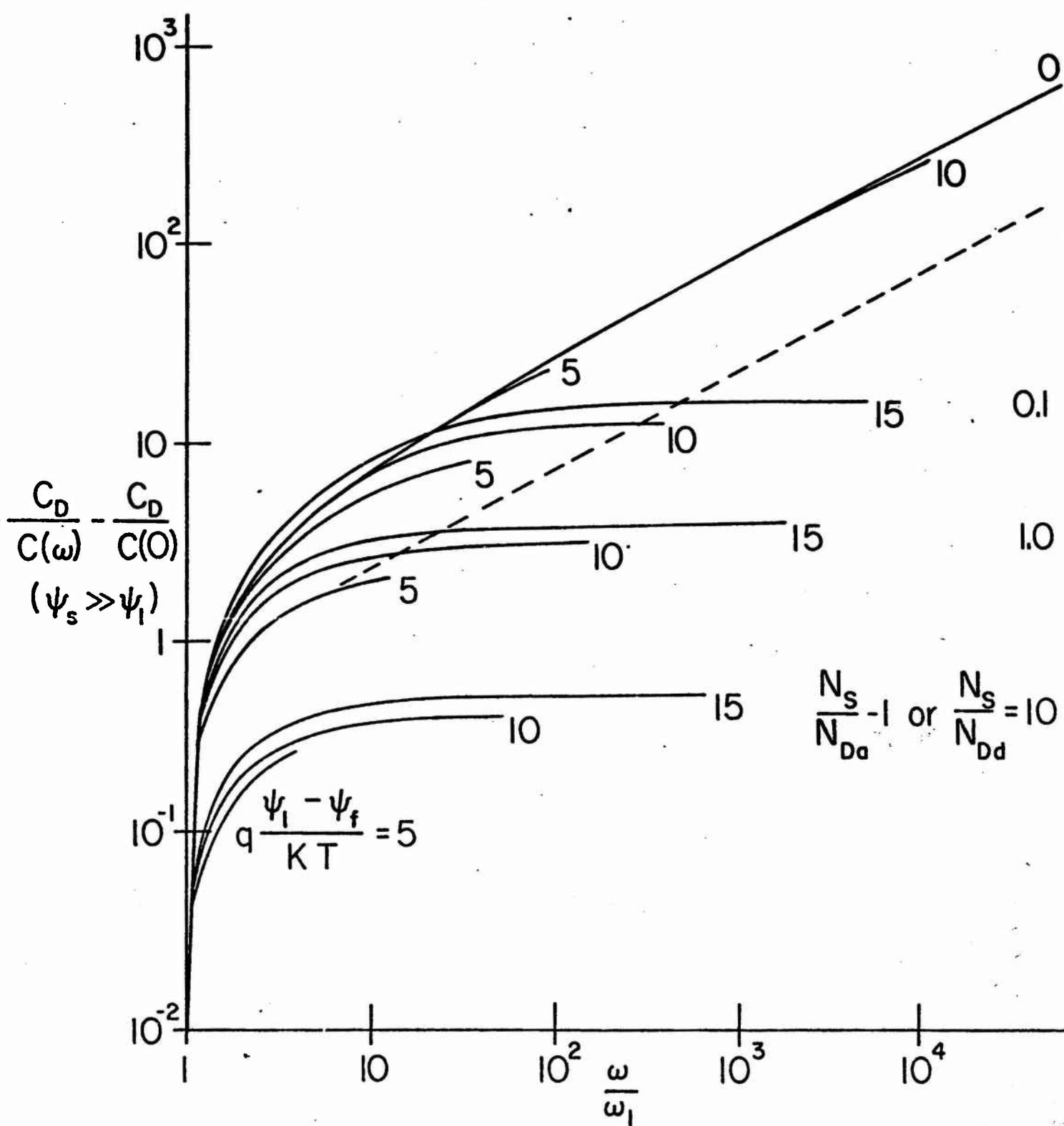
Figure 11. Normalized elastance difference between frequencies ω_1 and ω versus ω in units of ω_1 for selected degrees of freezeout $\left(\dfrac{q(\psi_1 - \psi_f)}{kT}\right)$ and ratio of shallow to deep impurity concentrations. The dotted line gives the asymptotic results of Schibli and Milnes (12) for the case of $N_s = 0$.
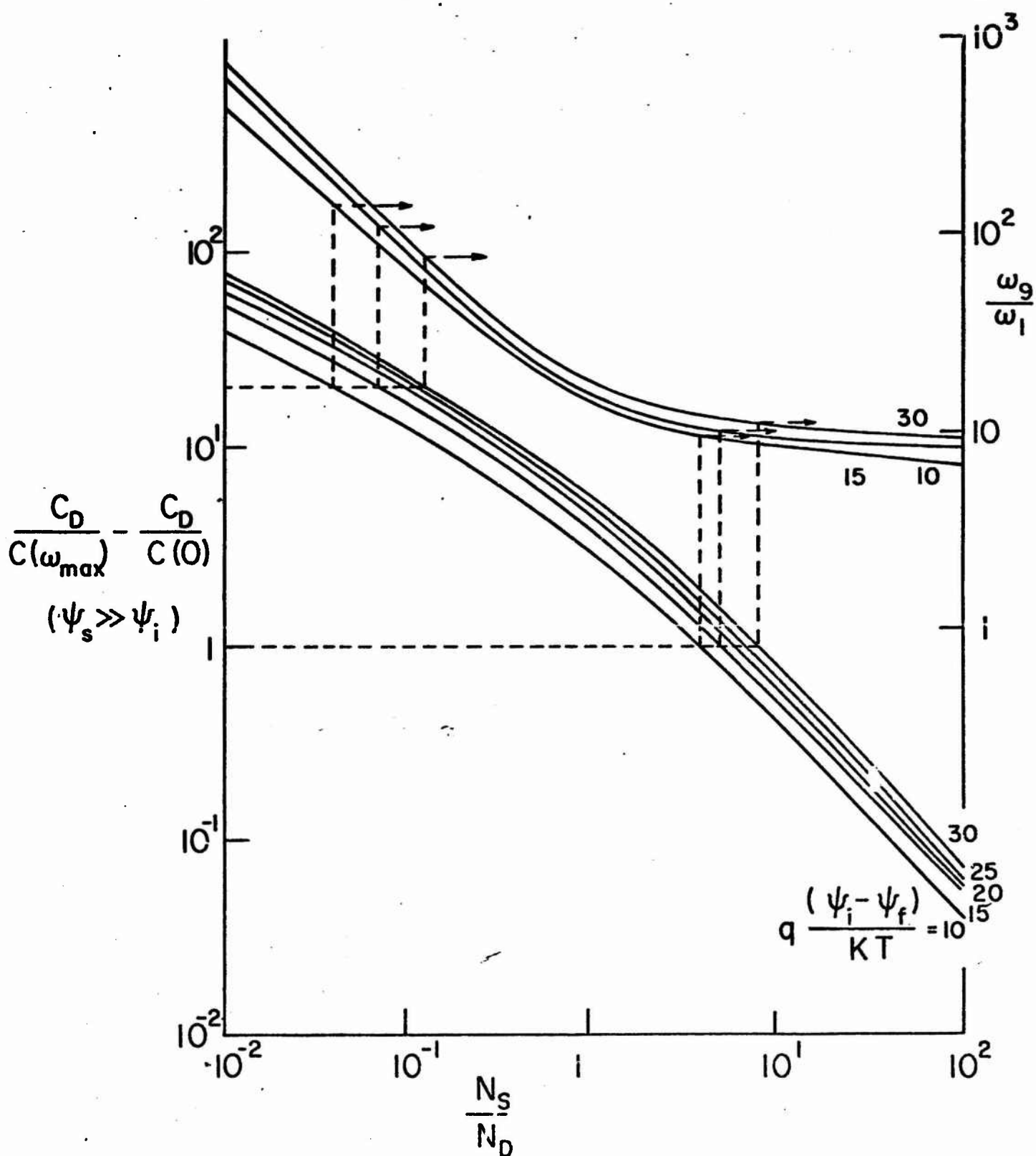
Figure 12. Maximum elastance (1/C) change and frequency interval for 90% of
of the maximum elastance change as a function of N_s/N_{d_d} for selected
degrees of impurity freezeout. Note the reversal of effects of freeze-
out when $N_s/N_{d_d} < 1$ or > 1 for a given elastance change.

level impurity from the capacitance-voltage relationship at a single temperature.

E. Experimental Techniques for Schottky-Barrier Capacitance-Voltage Studies

Development of an active capacitance probe front-end for a direct reading capacitance-voltage diagnostic system has been completed. Analysis of the behavior of active probe designs revealed a trade-off between minimum frequency of measurement and leakage current of the device under test. Experiments verified the existence of this trade-off. Several modifications of the unit were developed and a final design settled upon. The completed unit can measure capacitance with less than one percent error at frequencies below 10 Hz and with leakage currents as high as 100 μA.

Assembly is underway on the two remaining units in the system: (1) a universal constant-voltage signal source unit and (2) a general purpose logarithmic-algorithm analog computer unit. The signal source, when completed, will provide constant voltage sine-wave signals at two frequencies in the range 2 - 200 KHz, individually variable, with provision for amplitude and frequency modulation and sweep frequency generation. The unit will also provide automatic D-C bias sweeping.

The general purpose computer unit is near completion. When completed it will allow extreme flexibility of output format for capacitance-voltage (C-V) and capacitance-frequency (c-ω) measurement data. At first it will provide only data for impurity profile determination in materials. However, additional programming is being developed to allow presentation of C-V and C-ω data in formats previously requiring extensive calculation.

When completed, signals from the universal signal source will be applied to the device under test, mounted in the active probe unit.

-18-

The active probe unit output signals will then be analyzed by two lock-in amplifier units and peak detector units. Phase-sensitive amplification of the signals will be provided at this step, greatly reducing the effect of noise and sample leakage on the measurements. This feature is not available with bridge-type measurements. The output from the lock-in amplifiers will then be analyzed by the analog computer unit and the output plotted directly on an X-Y plotter.

The unit is scheduled for completion in the above form by June 1971. Projected extensions of the capabilities of the unit include (1) development of a variable temperature active probe unit for C-V and C-ω analysis, (2) development of active-probe units for current-voltage measurement, and (3) possible extension to digital output and control to allow further analysis of the measurement data by digital techniques.

F. Impurity Profiler

The distribution of electrically-active impurities in a semiconductor crystal is important both for meaningful characterization and also for controlled device fabrication. In order to understand and improve device performance one must know the doping concentration as a function of distance from the surface. It would be useful in fact to know the impurity profile after each device processing step.

One may often non-destructively measure carrier concentration profiles by means of Schottky-barrier C-V characteristics. We have designed and built an automatic "impurity profiler" based on these concepts[13].

For these measurements we first deposit a metal film by evaporation on the surface. The junction is contacted by a pointed probe. The back bias voltage across the barrier is then automatically swept and C-V data is automatically taken and processed by analog circuitry.

Figure 13 shows a profile of a GaAs epitaxial layer grown by the
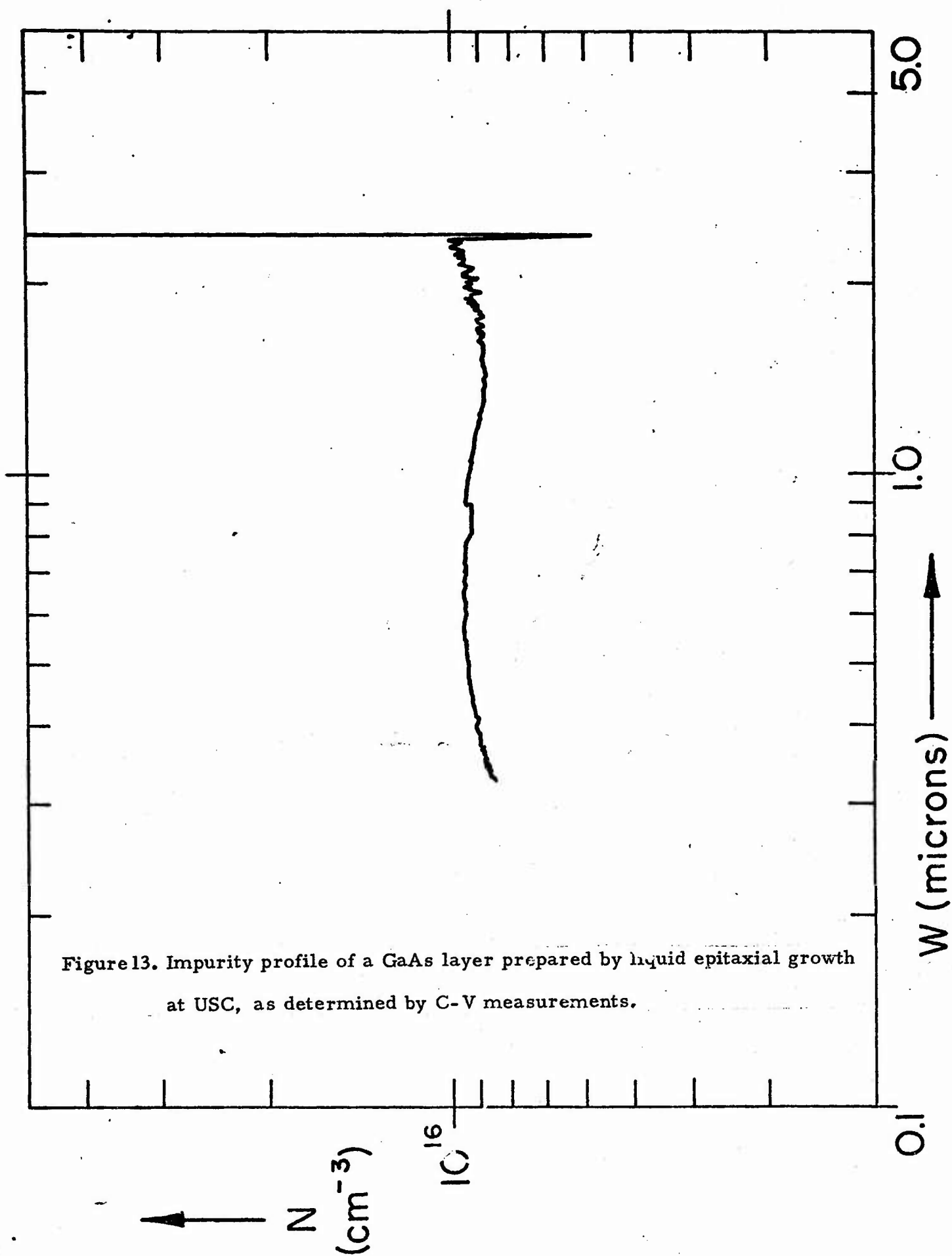
-19-

Figure 13. Impurity profile of a GaAs layer prepared by liquid epitaxial growth at USC, as determined by C-V measurements.

solution technique at USC. Figure 14 shows a profile of hyperthin vapor grown GaAs obtained from Monsanto; the epilayer is depleted before avalanche breakdown, and so the impurity gradient at the NN$^+$ interface is clearly seen.

By placing discs of metal film entirely across a slice, a radial variation in concentration profile can also be determined. In some cases, the profiler can also be used to evaluate bulk material.

G. Glow Discharge Spectroscopy for the Analysis of Thin Films

Available techniques for the chemical analysis of epitaxial semi-conductor films are limited due to typical sample thicknesses of 1-10 μm. The use of glow discharge spectroscopy was investigated as an analytical technique. GaAs was DC sputtered in argon and the glow discharge monitored for luminescence associated with one or more selected elements. The luminescent intensities combined with sputtering rates were used to estimate depth profile concentrations, e.g., the Sb concentrations in GaAs-GaSb alloy films on GaAs. The present detection limit for Sn in GaAs is 9×10^{17} atoms/cc for a sputtering rates of 1.4×10^{-5} cc/min. Sputtering yields have been measured over the range 0.5-3 kV and found to vary with orientation in the following order: (111)b, (111)a, (211), and (110).

H. Estimates of the Energy Gaps in Ga$_{1-x}$In$_x$As and GaAs$_{1-x}$Sb$_x$ Alloys from Photoluminescent Data

Photoluminescent spectra were measured in these alloys at room temperature and at the boiling points of helium and nitrogen. In general, the evidence was that impurity-band transitions were most likely for the detected luminescence. For both alloy systems the same dependence of the energy gap on x was observed as the values of $x \to 0$ (within estimated errors < 0.02 eV). Photoluminescent efficiencies of the alloys were encouragingly good, i.e., within a factor of 10 of solution-grown GaAs
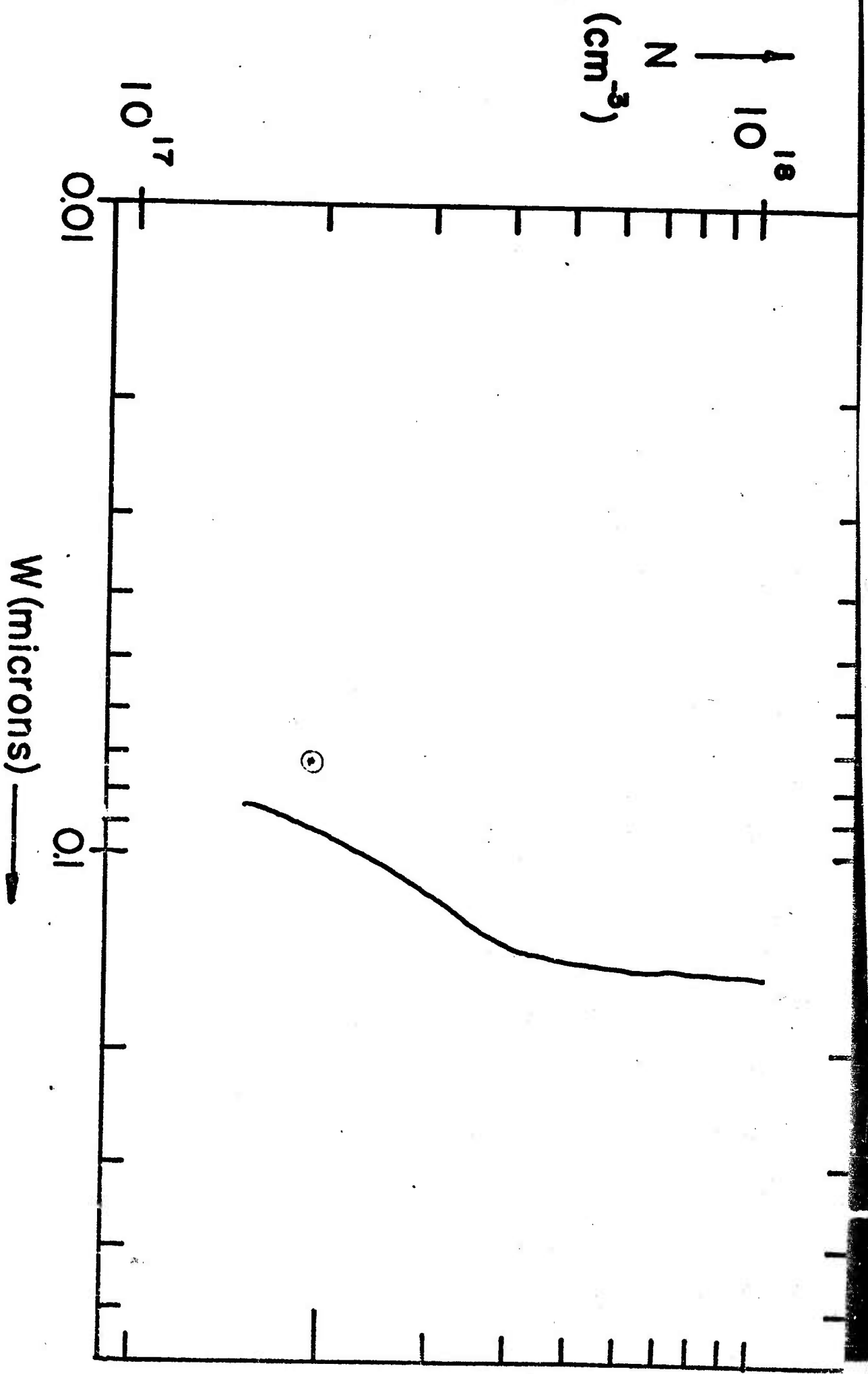
Figure 14 Impurity profile of hyperthin chemically vapor deposited epitaxial

film of GaAs from the Monsanto Company as determined by C-V

measurements.

for values of $x \leq 0.06$. Relative widths of the spectral and x-ray diffraction peaks were consistent with alloy homogeneities, $\Delta x/x$, of 0.1 or better. This is encouraging.

IV. DEVICES

Although useful devices are the ultimate goal of semiconductor research, the device portion of the present program is intended mainly as a test for the quality of our materials and the effectiveness of our crystal growth techniques.

A. Contacts and Heat Sinks

Fabrication of any semiconductor device ultimately requires reliable metal contacts to portions of the semiconductor. Reproducible formation of reliable contacts to GaAs appears to have been particularly elusive. We have developed a new technique yielding specific contact resistances as low as $\simeq 1 \times 10^{-5}$ ohm cm^{-2}. This figure refers to GaAs with $n = 1 \times 10^{18}$ cm^{-3}. The contacts are ohmic for electron concentrations in the GaAs of $< 10^{13}$ cm^{-3}. They can be made by sputtering of tin or by a relatively simple short circuit electroplating of tin from a $SnCl_2$-KCl-NH_4Cl salt bath on GaAs previously electroplated with gold. The other electrode of the molten salt short circuited cell is a Au-Sn alloy with the composition desired on the Au plated GaAs. It has been demonstrated that the average Au-Sn alloy compositions can be easily regulated to within 2%. One can thermocompression (TC) bond Au wires to these contacts. Required alloy temperatures are relatively low, 350-375°C.

A new method has been developed for assuring intimate contact between a device and a heat sink. It is applicable to Gunn devices, avalanche diodes, etc. A copper heat sink is electroplated onto the entire semiconductor slice. Diodes are fabricated by etching from the reverse side. Individual diodes are separated by sawing the copper into small squares.

For heat sinks or mechanical support, a thick metal layer is frequently desired. To have good thermal conductivity and to be strain free, the metal must be free of organic or chemical inclusions. We have

developed a new copper electroplating technique which accomplishes this. Prior to plating a metal film is deposited by vacuum evaporation. The first metal layer is selected for good ohmic contact and adhesion. The top layer is gold approximately 4000 $\overset{o}{A}$ thick. After wax mounting a 0.3 to 0.5 mil layer of gold is electrodeposited from a 24 karat neutral bath. A copper lead wire is attached to the gold surface. Copper is plated from a fluoborate bath without additives or from an acid bath. Temperature is 54 to 71°C and current density 1/2 to 1 ma/cm^{2}. The thermal resistances of platings from both baths are being measured.

B. GaAs Junction Field Effect Transistor (JFET)

The above improvements (II. E) in thin film growth have been used to grow n-type layers on p type GaAs substrates. The quality of the resulting pn junctions were excellent, as judged by low reverse biased leakage currents. Good junctions were associated with highly regular substrate-film interfacial surfaces. Growth conditions which compromised the regularity always resulted in p-n junctions with enhanced leakage currents. A mesa GaAs JFET with a ring-dot configuration was built to demonstrate the gate junction quality of GaAs transistors with relatively large transconductances (6×10^{-3} mhos).

Reverse currents at pinchoff voltages, ~ 12 v, were $\approx 2 \times 10^{-9}$ amp. Maximum processing temperatures required on the epitaxial films were under 430°C. This in part was due to the satisfactory performance of Au-Sn alloy contacts which were described previously.

C. Microwave Devices

We are presently fabricating microwave Schottky barrier detector and mixer diodes from Monsanto epitaxial material for later comparison with devices to be fabricated from materials produced at USC. Polishing techniques have been perfected, as noted in Section IIG. Capabilities for vacuum evaporation and chemical vapor deposition of thin films are being developed.

-23-

REFERENCES

1. V. W. Poch, Glastechnische Berichte 37, 533 (1964).

2.* V. Yip and W. R. Wilcox, Bull. Am. Phys. Soc. 15, 1624 (1970).

3.* R. J. Baughman, R. A. Lefever and W. R. Wilcox, J. Crystal Growth (in press).

4.* W. R. Wilcox and A. Leon, J. Crystal Growth (in press).

5. R. J. Walsh and A. H. Herzog, U.S. Pat. 3,170,273 (Feb. 23, 1965).

6. M. V. Sullivan and G. A. Kolb, J. Electrochem. Soc. 110, 585 (1963).

7. A. Reisman and R. Rohr, J. Electrochem. Soc. 111, 1425 (1964).

8.* C. R. Crowell, T. W. Kao and V. L. Rideout, Bull. Am. Phys. Soc. 15, 1615 (1970).

9. R. H. Fowler, Phys. Rev. 38, 45 (1931).

10. C. R. Crowell and S. M. Sze, J. Appl. Phys. 37, 2683 (1966).

11.* K. Nakano and C. R. Crowell, Bull. Am. Phys. Soc. 15, 1614 (1970).

12. E. Schibli and A. G. Milnes, Solid St. Electron. 11, 323 (1968).

13. B. J. Gorden and H. L. Stover and R. S. Hark in "Proceedings of the Symposium on Silicon Device Processing," American Society for Testing and Materials, 1970.

14.* J. E. Greene and J. M. Whelan, Bull. Am. Phys. Soc. 15, 1614 (1970).

15.* Y. Okuto and C. R. Crowell, "High Field Impact Ionization in the Baraff Approximation," Bull. Am. Phys. Soc. 15, 1615 (1970).

*Papers acknowledging ARPA support.